Electromagnetic Hydrodynamics of Liquid Crystals

P. Andrew Penz*
Scientific Research Staff, Ford Motor Company, Dearborn, Michigan 48121

and

G. W. Ford
Department of Physics, University of Michigan, Ann Arbor, Michigan 48104
(Received 10 November 1971)

We have developed a set of differential equations which describe the hydrodynamics of a conducting liquid crystal subjected to external electromagnetic fields. The mechanical forces resulting from the interaction of the fields with the liquid are expressed as operations on the Maxwell stress tensor. The use of this description allows a concise statement of the equations of motion. As an example of the validity of the formalism, we rigorously solve the boundary-value problem associated with the Williams domain (vortex) mode in nematic liquids. Using standard constitutive relations, physical boundary conditions, and experimentally measured material p-azoxylanisole constants, we quantitatively reproduce the significant experimental observations.

INTRODUCTION

The influence of electric and magnetic fields on liquid crystals has stimulated considerable interest in the past several years.[1-3] This type of investigation has proven fruitful because of the electromagnetic susceptibility exhibited by liquid crystals. We present a general theory of the coupled electromagnetic-hydrodynamic problem in a concise formalism involving the Maxwell stress tensor. The equations of motion, derivable from very general physical laws, are extensions of Cauchy's and Maxwell's equations. As such they are a mathematical formalism which requires constitutive relationships to describe physical problems. To illustrate the formalism, we treat the problem of the electric-field-induced vortex pattern (Williams domains) in a conducting nematic liquid crystal.[4]

GENERAL CONTINUUM HYDRODYNAMICS

The hydrodynamic equations applicable to liquid crystals have been known for some time.[5] Liquid crystals are unique liquids, since they are capable of transmitting stress couples and being subjected to body torques. Chistyakov gives a good review of the general physical characteristics of the liquid-crystal phase.[6] For instance, the nematic phase can be thought of as consisting of an aggregation of rod-shaped molecules whose axes tend to be parallel in macroscopic regions. This uniaxial direction is often represented by the term "director" $\vec{n}$, where $\vec{n}$ is a vector in the direction of the average molecular orientation. Since a nematic liquid resists spatial distortion of this orientation, stress couples can be present. The director can have a rotation apart from any fluid velocity, and thus an internal angular momentum is possible. Features such as these must be taken into account in the hydrodynamics of liquid crystals.

The equations of motion for a "polar" fluid can be derived in a standard way from conservation laws.[5] The conservation of mass yields the equation of continuity

$$\frac{D\rho}{Dt}+\rho(\nabla\cdot\vec{v})=0\,, \tag{1}$$

where ρ is the mass density, $\vec{v}$ is the fluid velocity, and D/Dt stands for the convective time derivative $\partial/\partial t+\vec{v}\cdot\nabla$. The conservation of linear momentum yields the force equation

$$\rho\frac{Dv_i}{Dt}=F_i+\frac{\partial\sigma_{ij}}{\partial x_j}\,, \tag{2}$$

where F_i is the ith component of any applied body force per unit volume and σ_{ij} is the stress tensor associated with the fluid. $\sigma_{ij}e_j\,dS$ is the ith component of the force on a surface element dS, where $\hat{e}$ is a unit vector along the normal to the surface outwards from the volume under consideration. Throughout this paper the repetition of an index implies summation over the three spatial indices x, y, and z. Care must be taken in comparing the hydrodynamic theories of liquid crystals. Some authors, for example, write the gradient of the stress tensor as $\partial\sigma_{ji}/\partial x_j$.[7]

The conservation of angular momentum for a liquid crystal does not follow directly from computation of the moment of linear momentum. As discussed above, a liquid crystal can have an intrinsic angular momentum per unit mass l_i and a stress couple C_{ij}. The conservation of total angular momentum leads to a torque equation:

$$\rho\frac{Dl_i}{Dt}=\tau_i-\epsilon_{ijk}\sigma_{jk}+\frac{\partial C_{ij}}{\partial x_j}\,, \tag{3}$$

where ϵ_{ijk} is the completely antisymmetric (Levi-Civita) tensor and τ_i is an applied body torque. The term $\epsilon_{ijk}\sigma_{jk}$ in Eq. (3) indicates the coupling between the stress tensor (e.g., the stress due to viscous flow) and the angular momentum change. In an isotropic fluid, l_i, τ_i, and C_{ij} are identically zero, thus requiring $\epsilon_{ijk}\sigma_{ij}=0$. It is important to note that conservation of total angular momentum for a liquid crystal does not require that σ_{ij} be symmetric, or equivalently $\epsilon_{ijk}\sigma_{jk}=0$. Angular momentum can be exchanged between the fluid flow system and the intrinsic system, etc. The question of the symmetry of σ_{ij} has received considerable attention in the recent literature.[8-10]

The conservation of energy leads to a power equation:

$$\rho\frac{DU}{dt}=\rho r-\nabla\cdot\vec{q}+\frac{\sigma_{ij}\,\partial v_i}{\partial x_j}+\frac{C_{ij}\,\partial\omega_i}{\partial x_j}+\epsilon_{ijk}\sigma_{jk}\omega_i\ , \qquad (4)$$

where r is the heat-supply function per unit mass per unit time, U is the internal energy per unit mass, $\vec{q}$ is the heat flow vector, and $\vec{\omega}$ is the angular velocity associated with the intrinsic angular momentum $\vec{I}$. For a nematic liquid crystal, the relationship would be $I\vec{\omega}=\vec{I}$, where I is a moment of inertia per unit mass. An example of the heat-supply function ρr would be the joule loss associated with drift current in an electric field.

MAXWELL STRESS TENSOR

We wish to apply the general hydrodynamic equations to a liquid crystal under the influence of an electromagnetic field. The problem of calculating ponderomotive forces on a fluid is not trivial. A precise derivation of these forces is given by Landau and Lifshitz.[11] If one assumes (i) isothermal conditions, (ii) a linear relation between the electric field $\vec{E}$ and the displacement field $\vec{D}$, and (iii) a similar relationship between the magnetic field $\vec{H}$ and the induction field $\vec{B}$, they show that the mechanical forces due to the electromagnetic field can be separated from the mechanical forces due to the medium in the absence of the fields. The electromagnetic forces can be most easily expressed as operations on the Maxwell stress tensor T_{ij}:

$$F_i=\frac{\partial T_{ij}}{\partial x_j}\ , \quad \tau_i=-\epsilon_{ijk}T_{jk}\ . \qquad (5)$$

Landau and Lifshitz show how T_{ij} is defined for an isotropic linear system. It is straightforward to extend this to an anisotropic linear system:

$$T_{ij}=E_iD_j-\tfrac{1}{2}\delta_{ij}\left(E_kD_k-\frac{\rho\epsilon_0E_kE_l\,\partial\epsilon_{kl}}{\partial\rho}\right)+H_iB_j-\tfrac{1}{2}\delta_{ij}\left(H_kB_k-\frac{\rho\mu_0H_kH_l\,\partial\mu_{kl}}{\partial\rho}\right)\ . \qquad (6)$$

The linear constitutive relations have been assumed to be $\vec{D}=\epsilon_0\overleftrightarrow{\epsilon}\cdot\vec{E}$ and $\vec{B}=\mu_0\overleftrightarrow{\mu}\cdot\vec{H}$, where the dielectric constant tensor is $\epsilon_0\overleftrightarrow{\epsilon}$ and the permeability tensor is $\mu_0\overleftrightarrow{\mu}$. Free energy considerations show that these tensors are symmetric. ϵ_0 and μ_0 are the permittivity and permeability of free space, respectively. We use the rationalized mks system of units. The terms involving ρ refer to electro- and magnetostriction.

A word of caution should be mentioned at this point. Numerous textbooks derive the Maxwell stress tensor in a vacuum or in an isotropic medium.[12] Various properties of the tensor are then shown, given these assumptions, e.g., T_{ij} is symmetric in an isotropic medium. These proofs do not necessarily carry over to the more general case under consideration here. Notice for example that a dielectric with an anisotropic dielectric tensor can experience a body torque $(\vec{P}\times\vec{E})_i=-\epsilon_{ijk}T_{jk}$, where $\vec{P}$ is the dipole moment per unit volume. The definitions of σ_{ij} and T_{ij} are somewhat arbitrary. The important physical point is that the equations of motion involve only the sum $\sigma_{ij}+T_{ij}$.

We wish to consider conducting liquid crystals and thus should discuss the validity of the previous equations for a medium with ionic conductivity. The hydrodynamic equations are completely general, including the case of a multicomponent fluid. In this case the fluid velocity becomes an average of the velocities of the different components, including ionic motion different from the average fluid velocity. A simple derivation of this result is given by Spitzer.[13] One can set up a Boltzmann equation for each of the individual fluid components, including collisions between components. When the average rate of momentum change is computed, Eq. (2) results. The collision terms resulting from collisions between components drop out by Newton's third law. Spitzer's analysis also shows the validity of the ponderomotive forces given by Eqs. (5) and (6). This multicomponent theory offers a direct interpretation of the heat-supply function r in terms of Ohmic loss. Finally a relation between E and j collision terms and various stress tensor gradients can be obtained.

We adopt the Maxwell field equations to complete the general equations of electromagnetic-hydrodynamics:

$$\nabla\cdot\vec{D}=\rho_e\ , \qquad \nabla\cdot\vec{B}=0\ , \qquad \nabla\times\vec{H}=\vec{j}+\frac{\partial\vec{D}}{\partial t}\ , \qquad \nabla\times\vec{E}=-\frac{\partial\vec{B}}{\partial t}\ , \qquad (7)$$

where ρ_e is the "true" charge density and $\vec{j}$ is the current density. The current density is not a Galilean invariant, and care must be taken to consider convection currents $(\nabla\cdot\vec{D})\vec{v}$, etc., when the medium described by Eq. (7) is in motion.[14] We intend to treat the electromagnetic problem only to

zeroth order in v/c, where c is the velocity of light. Thus the linear and angular momenta carried by the electromagnetic field can be ignored in Eqs. (2) and (3). The proper energy-balance equation [Eq. (4)] in the presence of an electromagnetic field is a difficult problem which we will treat in a subsequent paper.

CONSTITUTIVE EQUATIONS FOR NEMATIC MESOPHASE

In order to apply the general equations to specific problems, it is necessary to assume relationships between the various forces and responses, i.e., constitutive equations. We will outline the proper relations for nematic liquid crystals. As was discussed above, a nematic liquid can be described by a director $\vec{n}$ which we assume is of constant length:

$$|\vec{n}| = 1 \ . \tag{8}$$

The stress tensor can be broken into three parts,

$$\sigma_{ij} = -p\delta_{ij} + \sigma_{0ij} + \sigma'_{ij} \ , \tag{9}$$

where p is a hydrostatic pressure, σ_{0ij} is a stress due to elastic deformations of the liquid, and σ'_{ij} is a viscous component. It can be shown that[7]

$$\sigma_{0ij} = -\frac{\partial F}{\partial n_{kj}} n_{ki} \ , \tag{10}$$

where F is an elastic free energy and $n_{ij} = \partial n_i / \partial x_j$. Normally σ_{0ij} is quadratic in n_{ij} and can be ignored in linear treatments.

The viscous stress tensor σ'_{ij} has been derived by Leslie[7]:

$$\sigma'_{ij} = \alpha_1 n_k n_p A_{kp} n_i n_j + \alpha_2 n_j N_i + \alpha_3 n_i N_j + \alpha_4 A_{ij} + \alpha_5 n_j n_k A_{ki} + \alpha_6 n_i n_k A_{kj} \ , \tag{11}$$

where $\vec{\vec{A}}$ is the strain rate tensor

$$A_{ij} = \frac{1}{2}\left(\frac{\partial v_i}{\partial x_j} + \frac{\partial v_j}{\partial x_i}\right) \ ,$$

and $\vec{N}$ is

$$\vec{N} = \frac{D\vec{n}}{Dt} - \tfrac{1}{2}(\operatorname{curl}\vec{v}) \times \vec{n} \ .$$

Again there is an index interchange between Eq. (11) and Leslie's notation, arising from the divergence notation. The angular velocity of the director relative to the fluid is $\vec{n} \times \vec{N}$. The α's are constants with the dimension of viscosity and are not all independent. It has been shown that $\alpha_2 + \alpha_3 = \alpha_6 - \alpha_5$.[15] Given these constitutive relations for σ_{ij} and ignoring σ_{0ij}, it can be easily shown that the viscous contribution to the torque equation is given by

$$\epsilon_{ijk}\sigma_{jk} = \{\vec{n} \times [(\alpha_3 - \alpha_2)\vec{N} + (\alpha_6 - \alpha_5)\vec{\vec{A}}\vec{n}]\}_i \ . \tag{12}$$

We now consider the director torque $\partial C_{ij}/\partial x_j$. It can be shown that this torque arises from elastic forces opposing director distortion. This approach was pioneered by Frank.[16] Expressed in terms of a molecular field ($h_i = \delta F / \delta n_i$),

$$\frac{\partial C_{ij}}{\partial x_j} = [\vec{n} \times (\vec{h}_S + \vec{h}_T + \vec{h}_B)]_i + \epsilon_{ijk}\sigma_{0jk} \ , \tag{13}$$

where the various contributions (S, T, and B denote splay, torsion, and bend, respectively) are

$$\vec{h}_S = k_{11} \operatorname{grad} \operatorname{div}\vec{n} \ ,$$

$$\vec{h}_T = -k_{22}\{(\vec{n} \cdot \operatorname{curl}\vec{n}) \operatorname{curl}\vec{n} + \operatorname{curl}[(\vec{n} \cdot \operatorname{curl}\vec{n})\vec{n}]\} \ ,$$

$$\vec{h}_B = k_{33}\{(\vec{n} \times \operatorname{curl}\vec{n}) \times \operatorname{curl}\vec{n} + \operatorname{curl}[\vec{n} \times (\vec{n} \times \operatorname{curl}\vec{n})]\} \ ,$$

where the k's are appropriate elastic constants.

It is also necessary to postulate constitutive relations for the relative response tensors $\vec{\vec{\epsilon}}$ and $\vec{\vec{\mu}}$. If the director is assumed to determine the uniaxial direction,

$$\epsilon_{ij} = \epsilon_\perp \delta_{ij} + (\epsilon_\parallel - \epsilon_\perp) n_i n_j \ ,$$
$$\mu_{ij} = \mu_\perp \delta_{ij} + (\mu_\parallel - \mu_\perp) n_i n_j \ , \tag{14}$$

where $\epsilon_\parallel$ is the specific inductive capacity (dielectric constant) for the component of the electric field parallel to the director, $\mu_\parallel$ is the relative permeability parallel to the director, and $\epsilon_\perp$ and $\mu_\perp$ are the perpendicular components.

For a conducting medium it is necessary to postulate a constitutive relationship between the current density and the various forces that can produce the current flow in the fluid rest frame. Here we are dealing with a problem involving loss and intend to represent this feature in a steady-state approximation. This is certainly a good approximation for frequencies below the plasma frequencies associated with the ion.[13] Several forces can be thought of as influencing current flow[13]: electric fields, magnetic fields via the Lorentz force, and pressure and temperature gradients, although the latter would require a reformulation of the Maxwell stress tensor. In the interest of simplicity, we will treat only the current produced by an external electric field. In the Ohmic approximation $\vec{j} = \vec{\vec{\sigma}}_e \cdot \vec{E}$, where $\vec{\vec{\sigma}}_e$ is a conductivity tensor. Unfortunately convention requires us to use the same basic symbol for both the stress and conductivity tensors. We assume the conductivity tensor to be uniaxial, the orientation specified by the director $\vec{n}$:

$$(\sigma_e)_{ij} = \sigma_\perp \delta_{ij} + (\sigma_\parallel - \sigma_\perp) n_i n_j \ . \tag{15}$$

If one deals in a linear approximation, convection currents can be ignored.

It should be pointed out that there is a question of consistency between Eqs. (3) and (8). Equation (8) is a constraint on the three components of $\vec{n}$. Equation (3) seems to be three separate equations for the

three components of the torque and thus might violate the constraint of Eq. (8). Closer investigation reveals that the vector equation [Eq. (3)] has only components perpendicular to $\vec{n}$, i.e., it involves only two separate equations. Note that every term except $\epsilon_{ijk}T_{jk}$ involves a cross product with $\vec{n}$ [see also Eq. (12)]. It can be proven that given the constitutive equations of Eq. (14), $\epsilon_{ijk}T_{jk}$ has no component parallel to $\vec{n}$ (see Appendix A). Thus Eqs. (3) and (8) are consistent.

WILLIAMS DOMAIN MODE

In order to illustrate the utility of this theory, we have chosen to treat the electrohydrodynamic instability in nematic liquid crystals known as the Williams domain mode (WDM).[4] Extensive experimental and theoretical work has been performed on this problem,[17–21] due in part to the technological potential for display in the higher voltage regions.[1] We will review the basic experimental features here.

The experimental geometry is described by a capacitor filled with a nematic liquid crystal, typically p-azoxyanisole (PAA). The capacitor spacing d is usually in the 10–100-μ range, and at least one electrode is transparent to allow viewing of electro-optic phenomena. The capacitor faces are rubbed to promote orientation of the director in one direction in the absence of an electric field. We define

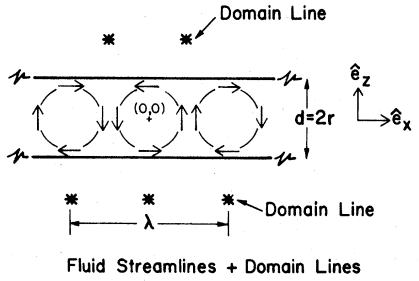

FIG. 1. Schematic drawing of the streamlines and domain lines is given (Ref. 20). The figure shows a cross section of the experimental geometry: a capacitor filled with liquid crystal. The electric field is applied in the z direction ($\hat{e}_z$), and the electrodes are rubbed to promote orientation of the director in the x direction ($\hat{e}_x$). Above a critical voltage, vortex motion is observed, the vortices extending in the y direction and antiparallel in adjacent cells. The periodicity of the fluid motion is λ and is roughly equal to $2d$, where d is the thickness of the sample. The origin of the coordinate system is taken to be at the center of the vortex in the middle of the drawing. When the sample is illuminated from below, an observer above the sample sees bright domain lines extending in the y direction. There are two sets of domain lines, one above the sample and one below the sample. The position of the bottom lines is under the center of the vortex motion, and the top lines are over the external part of the vortex flow.

a coordinate system by taking the x direction parallel to the rubbing direction and the z direction normal to the capacitor plates. Two striking phenomena occur when the sample is viewed in transmitted light with a sufficient voltage applied: (a) Bright lines appear running parallel to the y direction, and (b) the liquid is set into vortex motion. The observed features are diagramed schematically in Fig. 1. The domain lines are drawn under the assumption that the light is incident from below and the observer is viewing from above. The vorticity is antiparallel in adjacent domains. Experiments are generally done in temperature controlled environments. The power generated in the samples is typically on the order of a few mW per cm^3 at most (10^9-Ω cm resistivity). The conduction of the heat out of the sample would produce only an insignificant temperature difference. Thus it is safe to assume isothermal conditions prevail.

It has been shown that the domain lines can be interpreted as images of the microscope source.[20,21] The liquid crystal acts as a series of cylindrical lenses whose axes are in the y direction. The spatial distribution of the director consistent with both the real and virtual images are

$$\vec{n} = (\cos\theta,\ 0,\ \sin\theta)\ ,$$

$$\theta = \theta_1 \cos qx \cos(\pi z/d)\ .$$

This distribution is diagramed in Fig. 2 for $q = \pi/d$ and assumes that the origin of the coordinate system is at the center of one fluid vortex.

Two significant experimental observations are relevant to the theoretical treatment in this paper. Both concern the variation of the domain experiment with changes in the thickness d. As the sample thickness is changed (10–1000 μ), the voltage at which the domain pattern is first observed remains relatively constant (6–8 V for PAA). The spatial periodicity defined by q is found to vary roughly as $q = K/d$, where K is a constant on the order of π and is not strongly voltage dependent.

Two theoretical models have been proposed to explain these observations. One of the models involves the basic assumption of space-charge-limited (SCL) currents.[22,23] It has been shown that the conduction in the normal domain-mode experiment described is not SCL, and thus the basic phenomenon is not a SCL problem.[21] The other theory involves a treatment which reduces identically to Eqs. (13)–(20) of this paper. The theory is due to Helfrich and the rest of this paper should be regarded as an extension of Helfrich's treatment.[18] Helfrich's theory had one significant defect. He was forced to assume the relation $q \sim K/d$ in order to deduce the threshold voltage effect. We will show that this wave-vector-thickness relation is a natural result of the exact treatment of the boundary-value prob-

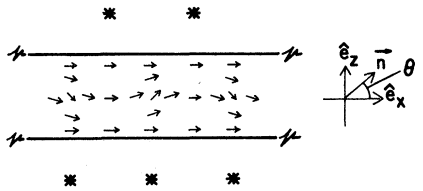

FIG. 2. Director orientation as deduced from domain lines. It can be shown that the domain lines are images of the incident light source (Refs. 20 and 21). The lines below the sample are virtual images, and the lines above the sample are real images. From the nature of the image pattern, it is possible to deduce the director orientation. The arrows in the figure represent the orientation of the director at the position of the arrow. Because of the anisotropy of the index of refraction, the liquid represents a series of cylindrical lenses which have constant thickness but a variation of optical path length in the x direction. The domain lines are shown in proper relation to the director pattern, i.e., the center of the director pattern represents an optical path minimum. As can be seen by reference to Fig. 1, the center of the director pattern also is the center of the vortex. Experimentally it is found that the focal length (position of domain line relative to sample midplane) of the lens system decreases as the voltage is increased above threshold. This can be interpreted as an increase in θ_1, the amplitude of the director distortion (Ref. 21).

lem.

Consideration of the experimental geometry reveals that the problem is essentially two dimensional in the xz plane. There is no variation in y. There are eight boundary conditions to be met. Since the sample plates have been rubbed to promote the director lying parallel to the plate, the angle θ must be zero at the plates:

$$\theta(z=\pm\tfrac{1}{2}d)=0\ . \tag{16}$$

Since the capacitor plates are good conductors relative to the liquid crystal, the electric field can have no x component at the sample plates:

$$E_x(z=\pm\tfrac{1}{2}d)=0\ . \tag{17}$$

The fluid must remain inside the plates, and thus

$$v_z(z=\pm\tfrac{1}{2}d)=0\ . \tag{18}$$

The fluid flow parallel to the plates must be zero at the plates to avoid infinite viscous loss:

$$v_x(z=\pm\tfrac{1}{2}d)=0\ . \tag{19}$$

Since there are boundary conditions in the x direction, it is not obvious that the periodicity in the x direction should be simply related to d. We show below that such a relation does exist.

THEORETICAL ANALYSIS OF DOMAIN PROBLEM

The fluid-field equations are obviously nonlinear equations. A standard theoretical method for finding approximate solutions to such equations is to linearize the problem by considering small oscillations away from equilibrium or steady state. In this case the zero-order state is described by the director being always parallel to the x direction and zero-flow velocity. We look for small oscillations away from this steady state. The linearization process leads to a set of differential equations which are translationally invariant for the infinite medium problem. It is well known that plane waves of the form $e^{i\vec{q}\cdot\vec{r}}$ form a complete set of functions for such a problem under normal conditions. The wave vector $\vec{q}$ will be represented by $(q_x, 0, q_z)$, since we will consider the problem to be spatially independent in the y direction. As usual, the small oscillation treatment leads to a dispersion relation between $\vec{q}$ and other physical parameters. If the dispersion relation is degenerate, the plane-wave representation must be expanded by multiplication by a polynomial in $\vec{r}$. Once the proper infinite medium solutions are obtained, they are used to satisfy the boundary conditions described above. The solution of this problem leads to the *normal modes* of the sandwich-capacitor system. The final result is obtained from the simultaneous solution of two characteristic equations, one for the infinite medium and one for the boundary-value problem.

The electric field is composed of the uniform applied field E_0 and a small distortion field of amplitude E_1 ($E_1 \ll E_0$):

$$\vec{E}=(0, 0, 1)E_0+(1, 0, q_z/q_x)\,e^{i\vec{q}\cdot\vec{r}}E_1\ . \tag{20}$$

Since $\nabla\times\vec{E}=0$, Maxwell's fourth equation is satisfied [Eq. (7)]. The velocity field is assumed to be

$$\vec{v}=(-q_z/q_x, 0, 1)\,e^{i\vec{q}\cdot\vec{r}}v_1\ , \tag{21}$$

where v_1 is sufficiently small that the convective portion of the time derivatives can be assumed to be zero. The velocity has zero divergence. Since the total time derivative of the mass density is zero, this form of the velocity satisfies the mass continuity equation [Eq. (1)]. We are treating an incompressible fluid. The angle of the director is also assumed to have a sinusoidal dependence with a small amplitude θ_1 ($\theta_1 \ll \pi$):

$$\theta=e^{i\vec{q}\cdot\vec{r}}\theta_1\ . \tag{22}$$

The director is thus given by

$$\vec{n}=(1, 0, e^{i\vec{q}\cdot\vec{r}}\theta_1)\ . \tag{23}$$

We assume that the magnetic fields produced by the currents are sufficiently weak with respect to other forces that all magnetic effects can be ignored. Consequently the magnetic components of Eqs. (6) and (7) do not place any constraint on the problem. This amounts to ignoring the Lorentz force due to the current in one part of the sample

acting on the current in another part of the sample. For currents typically on the order of microamperes and sample areas on the order of 1 cm^2, this is certainly a good approximation.

Implicit in Eq. (7) is the conservation of charge equation

$$\frac{\partial \rho_e}{\partial t} + \nabla \cdot \vec{j} = 0 \ . \tag{24}$$

In the steady-state condition, this means that the divergence of the current density must vanish. Thus for this particular problem, the solution of Maxwell's first and third equations reduces to the solution of Eq. (24).

Given the form of $\vec{n}$, the various susceptibility tensors can be written in the laboratory frame. It is instructive to produce the conductivity tensor consistent with Eq. (14):

$$\overleftrightarrow{\sigma}_{e\,\mathrm{lab}} = \begin{pmatrix} \sigma_{\parallel} & 0 & (\sigma_{\parallel} - \sigma_{\perp})\theta_1 e^{i\vec{q}\cdot\vec{r}} \\ 0 & \sigma_{\perp} & 0 \\ (\sigma_{\parallel} - \sigma_{\perp})\theta_1 e^{i\vec{q}\cdot\vec{r}} & 0 & \sigma_{\perp} \end{pmatrix} . \tag{25}$$

From Eq. (25) it is clear that the conductivity tensor has off-diagonal elements for nonzero θ_1. It is well known that this situation leads to electric fields transverse to the current, e.g., the Hall voltage in the case of conductors in a magnetic field. This transverse field can be thought of as the result of a space charge. The interaction of the space charge with $\vec{E}_0$ produces the domain mode.

The choice of $\vec{E}$, $\vec{v}$, and $\vec{n}$ given in Eqs. (20)–(23) satisfy all the relevant fluid-field equations except Eqs. (2), (3), and (24). In order to solve the equations of linear and angular momentum conservation, we need the expressions for σ_{ij} and T_{ij} consistent with these assumptions. This is a tedious algebraic problem, and we see little utility in reproducing all the various steps. Instead we will derive T_{xx} and σ_{xx}.

The definition of T_{xx} is $\frac{1}{2}E_xD_x - \frac{1}{2}E_zD_z$ when electrostriction and magnetic field effects are ignored. Formation of the product $\epsilon_{ij}E_j$ reveals that

$$D_x = \epsilon_0\epsilon_{\parallel}E_1 e^{i\vec{q}\cdot\vec{r}} + \epsilon_0(\epsilon_{\parallel} - \epsilon_{\perp})\theta_1 E_0 e^{i\vec{q}\cdot\vec{r}}$$

and

$$D_z = \epsilon_0\epsilon_{\perp}E_0 + \epsilon_0\epsilon_{\perp}SE_1 e^{i\vec{q}\cdot\vec{r}} ,$$

where $S \equiv q_z/q_x$. The product E_xD_x contain terms proportional to E_1^2 and $E_1\theta_1$. We intend to linearize the problem in the distortion amplitudes and so equate E_xD_x to zero. E_zD_z contains zeroth-, first-, and second-order terms. Again dropping the second-order term,

$$T_{xx} = -\tfrac{1}{2}\epsilon_0\epsilon_{\perp}(E_0^2 + 2SE_0E_1e^{i\vec{q}\cdot\vec{r}}) .$$

Naturally the driving amplitude E_0 is considered a zeroth-order term.

The definition of σ_{ij} is given by Eqs. (9)–(11). As was stated above, it is generally assumed that σ_{0ij} can be ignored in a first-order treatment. Also we assume that the α_1 term in σ'_{ij} is sufficiently small that it can be ignored with respect to the $\alpha_2 \cdots \alpha_6$ terms. This assumption is expedient since α_1 has not been measured accurately, and including that it complicates the theory considerably. We assume the pressure to be of the form $p = p_0 + p_1 e^{i\vec{q}\cdot\vec{r}}$, with these restrictions

$$\sigma_{xx} = -p + (\alpha_2 + \alpha_3)n_xN_x + \alpha_4A_{xx} + (\alpha_5 + \alpha_6)(n_x^2A_{xx} + n_xn_zA_{zx}) .$$

The case of the velocity distribution given in Eq. (21) permits the calculation of the A_{ij} and N_i components [Eq. (11)]:

$$A_{xx} = -iq_zv_1e^{i\vec{q}\cdot\vec{r}} , \quad A_{zx} = \tfrac{1}{2}iq_x(1 - S^2)v_1e^{i\vec{q}\cdot\vec{r}} ,$$

and

$$N_x = \tfrac{1}{2}iq_x(S^2 + 1)\theta_1v_1e^{i2\vec{q}\cdot\vec{r}} .$$

The assumption of linearity in distortion amplitudes means that we can set N_x equal to zero. Since the $n_xn_zA_{zx}$ term in the σ_{xx} expression goes as θ_1v_1, we ignore this term also. It follows that to first order $\sigma_{xx} = -p - (\alpha_4 + \alpha_5 + \alpha_6)iq_zv_1e^{i\vec{q}\cdot\vec{r}}$.

We are now ready to proceed with the fluid-field equations that have yet to be considered. The x component of the linear momentum equation [Eq. (2)] reduces to

$$p_1 + \frac{1}{2}\left(\frac{q_z^3}{q_x}(\alpha_3 + \alpha_4 + \alpha_5) + q_z(\alpha_3 + \alpha_4 + 2\alpha_5 + \alpha_6)\right)v_1 = 0 . \tag{26}$$

The y component of Eq. (2) is identically zero and the z component reduces to

$$-iq_zp_1 + \tfrac{1}{2}[(\alpha_2 - \alpha_4 + \alpha_5)q_z^2 + (\alpha_2 - \alpha_4 - \alpha_5)q_x^2]v_1 + iE_0\epsilon_0\left(\epsilon_{\perp}\frac{q_z^2}{q_x} + \epsilon_{\parallel}q_x\right)E_1 + iq_x(\epsilon_{\parallel} - \epsilon_{\perp})\epsilon_0E_0^2\theta_1 = 0 . \tag{27}$$

The only nonzero component of the torque equation is the y component

$$+i\left(-\alpha_3\frac{q_z^2}{q_x} + \alpha_2q_x\right)v_1 - \epsilon_0(\epsilon_{\parallel} - \epsilon_{\perp})E_0E_1 + [q_x^2k_{33} + q_z^2k_{11} - \epsilon_0(\epsilon_{\parallel} - \epsilon_{\perp})E_0^2]\theta_1 = 0 . \tag{28}$$

The charge continuity equation reduces to

$$(\sigma_{\perp}q_z^2/q_x^2 + \sigma_{\parallel})E_1 + (\sigma_{\parallel} - \sigma_{\perp})E_0\theta_1 = 0 . \tag{29}$$

Equations (26)–(29) are a set of linear homogeneous equations in the amplitudes p_1, v_1, E_1, and θ_1. It is well known that such a set of equations

can be solved simultaneously if and only if the determinant of the coefficients is zero. This condition leads to a "dispersion relation" between S and E_0/q_x for the infinite medium problem:

$$0=(S^2+1)\left((\alpha_2-S^2\alpha_3)\frac{\epsilon_0 E_0^2}{q_x^2}(\sigma_\perp\epsilon_\parallel-\sigma_\parallel\epsilon_\perp)\right.$$
$$\left.-(\eta_2+S^2\eta_1)\left[(k_{33}+S^3k_{11})(\sigma_\parallel+S^2\sigma_\perp)-\frac{\epsilon_0E_0^2}{q_x^2}(\epsilon_\parallel-\epsilon_\perp)\sigma_\perp(1+S^2)\right]\right), \tag{30}$$

where $S=q_z/q_x$, $\eta_2=\frac{1}{2}(-\alpha_2+\alpha_4+\alpha_5)$, and $\eta_1=\frac{1}{2}(\alpha_3+\alpha_4+\alpha_6)$.[24] Equation (30) is an eighth-order algebraic equation in S or a fourth-order equation in S^2. Fortunately, two of the roots are readily apparent, as $S=\pm i$ (note that this is due to the assumption that $\alpha_1=0$). The problem is then to solve the remaining cubic equation in S^2. This equation can be rewritten as

$$\epsilon_0\left(\frac{E_0}{q_x}\right)^2=\frac{k_{33}+S^2k_{11}}{(\alpha_2-S^2\alpha_3)/(\eta_2+S^2\eta_1)\,(\sigma_\perp\epsilon_\parallel-\sigma_\parallel\epsilon)/(\sigma_\parallel+S^2\sigma_\perp)+(\epsilon_\parallel-\epsilon_\perp)\sigma_\perp(1+S^2)/(\sigma_\parallel+S^2\sigma_\perp)}\ . \tag{31}$$

Equation (31) has been presented for comparison with Helfrich's theory.[18] It can be seen that the special case of $S=0$ is *exactly* his result. It should be noted that Helfrich's treatment interchanged the standard definitions of η_2 and η_1.

While analytic formulas do exist for the general solution of a cubic equation, the formulas are not practical considering the complexity of the coefficients in Eq. (31). We thus have chosen to solve the problem numerically using a digital computer. For typical values of the parameter $(E_0/q_x)^2$, we calculated the other six values of S_β using experimental values for all the material constants (see Appendixes B and C for the values used in the calculation). It should be emphasized that there are no adjustable parameters in this treatment. Note that the eight S_β values come in $\pm$ pairs.

Eight different wave vectors are possible: $\vec{q}_\beta=(q_x,\ 0,\ S_\beta q_x)$. Since we also have eight boundary conditions [Eq. (16)–(19)] to satisfy, it is in principle possible to solve the boundary-value problem. For example consider the boundary condition on the z component of the velocity:

$$v_z(z=+\tfrac{1}{2}d)=\left\{\begin{matrix}v_Ae^{iS_1\varphi}+v_{-A}e^{-iS_1\varphi}+v_Be^{iS_2\varphi}+v_{-B}e^{-iS_2\varphi}\\+v_Ce^{iS_3\varphi}+v_{-C}e^{-iS_3\varphi}+v_De^{iS_4\varphi}+v_{-D}e^{-iS_4\varphi}\end{matrix}\right\}e^{iq_xx}=0\ ,$$

where v_A, v_{-A}, v_B, v_{-B}, etc., are the arbitrary coefficients to be determined by the boundary conditions and $\frac{1}{2}q_xd=\varphi$. There are similar expressions for v_z evaluated at $z=-\frac{1}{2}d$. v_x, E_x, and θ follow the same pattern. Again it does not appear profitable to reproduce all these equations. One must solve another set of linear homogeneous equations, and the boundary-value determinant (BVD) associated with these equations must be zero for a solution to be possible. The symmetry between the boundary conditions at $z=\pm\frac{1}{2}d$ and the symmetry of the S values coming in positive/negative pairs allows one to reduce the set of eight equations to two independent sets of four equations. Solutions to the problem will occur when either one or both of the two 4×4 determinants are zero. We reproduce one of the two determinant equations below:

$$0=\begin{vmatrix}\cos S_1\varphi & \cos S_2\varphi & \cos S_3\varphi & \cos S_4\varphi\\ S_1\sin S_1\varphi & S_2\sin S_2\varphi & S_3\sin S_3\varphi & S_4\sin S_4\varphi\\ M_1\cos S_1\varphi & M_2\cos S_2\varphi & M_3\cos S_3\varphi & M_4\cos S_4\varphi\\ M_1N_1\cos S_1\varphi & M_2N_2\cos S_2\varphi & M_3N_3\cos S_3\varphi & M_4N_4\cos S_4\varphi\end{vmatrix}\ , \tag{32}$$

where

$$M_\beta=\frac{1-S_\beta^2\alpha_3/\alpha_2}{[(S_\beta^2+k_{33}/k_{11})(S_\beta^2+\sigma_\parallel/\sigma_\perp)+(\epsilon_0E_0^2/q_x^2k_{11})(\epsilon_\perp-\epsilon_\parallel)(1+S_\beta^2)]}\ ,\qquad N_\beta=(\sigma_\perp S_\beta^2+\sigma_\parallel)/\sigma_\perp\ .$$

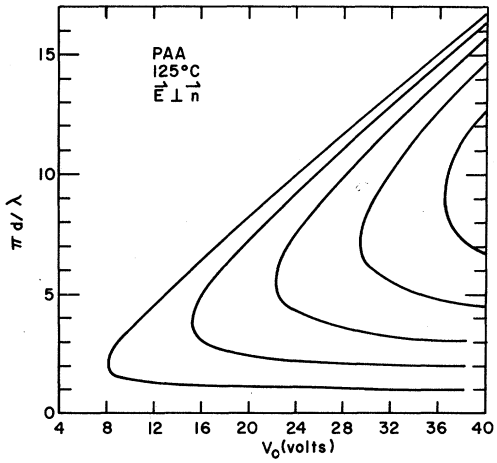

FIG. 3. Computer calculation of the normal-mode wave vectors for PAA. The lowest-voltage curve in the figure represents the only values of voltage and phase for which Eqs. (31) and (32) are first simultaneously satisfied. The next-higher-voltage curve represents those values for which Eq. (31) and the dual of Eq. (32) are satisfied. Additional curves appear at even larger values of V and $\pi d/\lambda$, reflecting the sinusoidal nature of the functions in Eq. (32). The fact that no solutions exist below 8 V indicates that the domain mode has a critical voltage. The phase for each solution is double valued for a given voltage. It is argued in the text that the first low-phase solution represents the WDM and the first high-phase solution describes the VGM. The calculations have been based on experimentally determined material coefficients (Appendix B). The 8-V threshold prediction compares well with the experimental values of 6–8 V. The curve beginning at 8 V represents one vortex layer and each higher-voltage dispersion relation describes an additional layer of vortices added to the sample. These curves were calculated using a linearized theory. Nonlinear effects could alter the detailed shapes at higher voltages.

The dual BVD equation is obtained by interchanging sines and cosines in Eq. (32).

Equation (32) is a relation between φ and V_0. There is the obvious φ dependence with S_β, M_β, and N_β depending on V_0/φ. This relationship is the final solution to the WDM problem. The boundary value problem can be solved for only certain values of q_x given V_0. These values of q_x determine the normal modes of the system. Helfrich was forced to assume a q_x to derive a critical voltage because he did not attempt a boundary-value solution.[18] The boundary-value problem is the key step in the proof of a critical voltage, as we now show.

NUMERICAL ANALYSIS

The numerical solution of Eqs. (31) and (32) is straightforward. We have chosen not to reproduce the program but will describe briefly the significant features. (A copy of the program, written in FORTRAN IV, can be obtained by request.) Note that the electric field appears explicitly only in Eq. (30) in the form $E_0/q_x = V_0/2\varphi$. The sample thickness appears only in Eq. (32) in the form $\varphi = \frac{1}{2}q_x d$. It is convenient mathematically to set V_0 and d, and then vary q_x by varying φ. The program begins by choosing V_0 and φ, and then calculating the various ratios S_β. In general the S_β's can be complex, but the nature of Eq. (30) insures that the complex roots come in complex conjugate pairs. The calculated S values are substituted into the BVD [Eq. (32)], and a value for this quantity is obtained. The complex conjugate nature of the S_β^2 roots insure that the BVD is either pure real or pure imaginary. For an arbitrary choice of V_0 and φ, the BVD is, in general, not zero, i.e., an arbitrary point in the V_0, φ plane does *not* represent a solution of the boundary-value problem. Another value of φ is chosen and the process is repeated using the same V_0. A solution of the problem results if the BVD changes sign by going through zero between two chosen ϕ's. A new value of V_0 is chosen and the process is repeated. In this manner, those combinations of (V_0, φ) for which Eqs. (31) and (32) are simultaneously zero can be determined.

The results of these calculations are shown in Fig. 3 for PAA at 125 °C. The phase-voltage plot shows five distinct curves along which the liquid crystal can have electrohydrodynamic modes. The first curve begins at a threshold voltage of 8.2 V, and $\frac{1}{2}q_x d$ is double valued as a function of V_0. We will refer to this curve as possessing a low and a high φ branch. We would like to again emphasize that the value of 8.2 V is a number which follows directly from the empirical material constants listed in Appendix B. Another double-valued solution begins at 15.3 V. This solution comes from the dual of Eq. (32), i.e., sines interchanged with cosines in Eq. (32). At still higher voltages, a similar nest of curves is found with each solution beginning at roughly an integer value of 8.2 V. These additional solutions occur because of the periodicity of the sinusoidal functions in Eq. (32).

COMPARISON OF THEORY AND EXPERIMENT

We do not intend to treat the questions of stability or nonlinearity in this paper. Thus we cannot rigorously predict which portion or portions of Fig. 3 correspond to physical reality. It is abundantly clear, however, that the low φ branch of the first solution describes the WDM experimental situation. *First* there is the existence of a critical or threshold voltage. The voltage at which the domain mode appears is unambiguously predicted to be independent of thickness. *Second*, there is the prediction that at any one voltage the phase factor is independent of thickness, or equivalently $q_x \propto 1/d$. *Third*, there is the prediction, revealed

by the lower branch of the first solution, that q_x will not be a strongly dependent function of V_0. As we discussed above, these are the three significant qualitative features associated with the experimental observations of domains.

In order to evaluate the quantitative predictions of the theory, it is necessary to discuss the experimental uncertainty associated with the material constants in Appendix B. The quantity with the largest experimental uncertainty is $\sigma_{\parallel}/\sigma_{\perp}$. The reference paper for this ratio only estimates this number and so we should certainly expect a ±20% uncertainty. It should also be noted that the viscosities were measured at a slightly different temperature than the other parameters. Given the complexity of the calculation, it is not trivial to estimate the uncertainty to be expected in the predicted threshold voltage as a result of the experimental uncertainties. A reasonable estimate would be ±30%, due mainly to the conductivity ratio estimate. A similar estimate would be in order for the value of the phase factor.

Given these qualifications, there seems to be quite good agreement between the quantitative features of the theory and experiment. The predicted threshold voltage is 8 ± 2 V. The observed low-frequency values for V_0 are in the 6–8 V rms range. We must restrict this analysis to specifically exclude the zero frequency case due to the difficulties of electrode polarization, etc.[21] At dc there are serious questions about the Ohmic assumption and the electric field boundary condition. At frequencies near the space-charge relaxation frequencies, other features play an important role.[25–27]

A quantitative comparison can be made between the experimental and theoretical value of the phase factor $\frac{1}{2}q_x d$. Experimentally this number, measured above threshold, has a value of approximately 2.[20] In the same voltage range, the theoretical prediction from the lower branch of the first solution is between 1.2 and 1.4. Certainly there is better than an order of magnitude agreement, although the theoretical estimate of ±30% uncertainty does not quite include the experimental value. Considering the complexity of the assumptions made and the experimental uncertainties, we are satisfied with this degree of quantitative agreement.

In order to further investigate the two branches of the first "dispersion" curve, we have calculated the z dependence of the four functions associated with the boundary conditions. Since we have treated the problem in a linear approximation, the amplitude of the distortions are still unknown to within a common multiplicative factor. This is the standard solution of linear homogeneous equations. We plot in Fig. 4 the dependence at $x=0$ of the functions $-v_x$, $-e_x$, and θ; the function v_z is plotted at $x=\pi/q_x$. The figure is computed for a solution on the low branch at $V_0=9.6$ V and $\varphi=1.488$. Inspection will reveal that the computed variations of v_z, $-v_x$, and θ match exactly with the qualitative experimental observations given in Figs. 1 and 2 and with the experimental observation of roughly solid-body rotation in the centers of the vortices.[20] Again we emphasize that the ordinates in Fig. 4 are not absolute. Each is

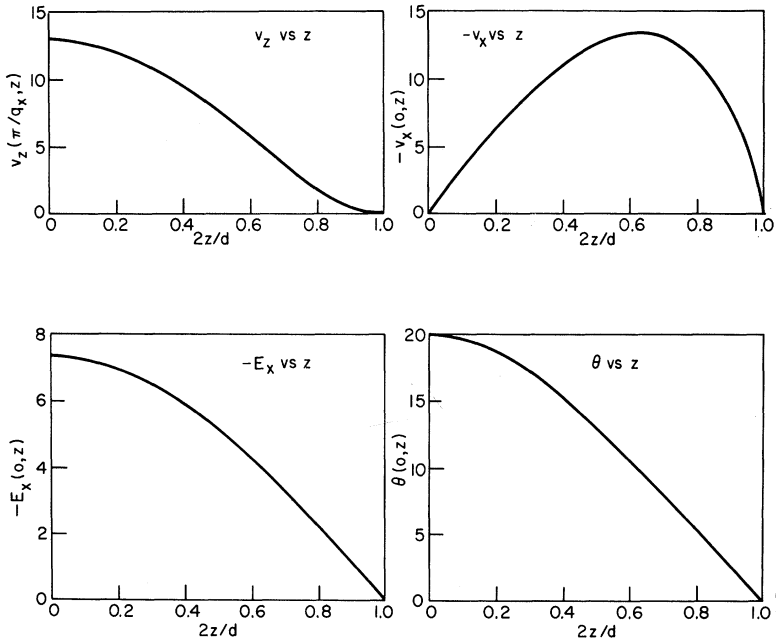

FIG. 4. Computer calculations of the relative distortion amplitudes as a function of z for the $V=9.6$, $\varphi=1.488$ solution. The z component of velocity is calculated as $x=\pi/q_x$, while the other three are calculated at $x=0$. Inspection of the v_z, $-v_x$, and θ plots shows that they are exactly the variation indicated in Figs. 1 and 2. The $-E_x$ plot can be seen to be correct by the following argument. Since fluid is moving up at π/q_x and down on $-\pi/q_x$, there must be positive space charge at π/q_x and negative space charge at $-\pi/q_x$ (the electric field has been set in the positive z direction). This means that E_x due to this space charge must point in the negative x direction at $x=0$. All the plots are relative to an undetermined distortion amplitude v_A as is usual in the solution of homogeneous equations. To obtain the absolute values of v_z, $-v_x$, $-E_x$, and θ, multiply the ordinates in the figure by v_A, v_A, $(\sigma_{\parallel}-\sigma_{\perp})/\sigma_{\perp})(E_0/k_{11}q_x)\alpha_2 v_A$, and $-(\alpha_2/k_{11}q_x)V_A$, respectively.

undetermined by a constant amplitude factor v_A which must be determined by nonlinear analysis. To obtain the absolute value of v_z, v_x, e_x, and θ, multiply the corresponding ordinate by v_A, v_A, $[(\sigma_\parallel - \sigma_\perp)/\sigma_\perp]\,(E_0/k_\parallel q_x)\;\alpha_2 v_A$, and $-\alpha_2 v_A/k_{11}\,q_x$, respectively.

The high φ solution in Fig. 3 can also be identified with an experimentally observed mode. Note that the high-φ solution corresponds to a linear dependence of φ on V_0 at higher V_0 values. Greubel and Wolff[28] report that very thin samples with low conductivity produce a mode with just such a φ, V_0 relationship. Vistin[29] has also reported similar observations. This mode is of technological interest because the domain lines are sufficiently close together to form a diffraction grating for visible light. Since the line spacing can be adjusted with the electric field, the liquid crystal operates in what might be called a variable grating mode (VGM). Unfortunately the material constants are not available for the nematic liquid crystals (NLC) used in the experiments. The slope of the V_0, φ linear region for PAA, is in order of magnitude agreement with that of the experimental material. The steady-state nature of our theory precludes a prediction about the conditions under which the low- and high-φ solutions will be stable. A stability treatment would be guided by the fact that thin low-conductivity samples prefer the VGM. Thick high-conductivity samples prefer the WDM. While linear combinations of the two modes appear to be possible in theory, they are not observed in practice. Since the calculations were performed using a linearized theory, nonlinear effects may alter the shape of Fig. 3. Experiments have shown[21] that θ_1 is limited to 45°, and so the linear theory should be fairly representative of the experiments.

We now wish to consider the significance of the additional dispersion relations shown in Fig. 3. We have calculated the velocity spatial distributions consistent with each of these modes. The mode which begins at 15 V has a velocity profile indicated schematically in Fig. 5. The pattern is still one of antiparallel vortices, this mode having two layers of vortex motion. Each succeeding mode of Fig. 3 has an additional layer of vortices. For instance, the mode beginning at 36 V has five layers.

It is well known in the field of stability analysis that turbulence may be expected when a stationary solution of the hydrodynamic equations has superposed on it a nonsteady small perturbation.[30] On such experience we can base a conjecture that turbulence might arise at 15.3 V (see Fig. 3, second solution). In some sense, the two vortex motions of Figs. 1 and 5 will compete to establish their own dominance. There is, of course, an experimentally observed turbulence.[31] The name dynamic scattering mode has been coined to describe this phenomenon. Certainly this mathematical occurrence of zeros in both Eq. (32) and its dual should be considered as a possible explanation of the onset of this turbulence. The explanation for the turbulence is most important because it is the turbulence which makes the system practical for display applications.

There are a number of other agreements between experimental observations and predictions made following this line of reasoning, e.g., frequency, temperature, and impurity dependence. For further discussion of these factors, see Refs. 18 and 20.

While PAA was the prototype NCL for many years, a room-temperature nematic has recently become quite popular. This material is p-methoxy-n-p-benzilidene butylaniline (MBBA). In Fig. 6 we present the results of calculations for MBBA using the material constants listed in Appendix C. The qualitative nature of the dispersion curves for PAA and MBBA is the same. The WDM and VGM regions of the MBBA figure are apparent, and dispersion relations for one, two, and three layers of vortex motion are shown. The predicted critical voltage for the one layer mode is 6.9 V. The Orsay Liquid Group[26] has observed an electrohydrodynamic instability at 5 V in MBBA. Their picture of this mode shows a y dependence of the domain lines, however, and so an exact comparison with our theory of uniform lines in the y direction is not possible. There is also the problem that a true dc experiment is complicated by electrochemical reactions at the electrodes. It may be true, however, that a more complicated domain pattern containing a y variation has a lower critical voltage than the 6.9 V we predict for our model.

While the basic mathematical solution has been presented, the physical origin of the domain mode may not be too clear. The basic ideas were first

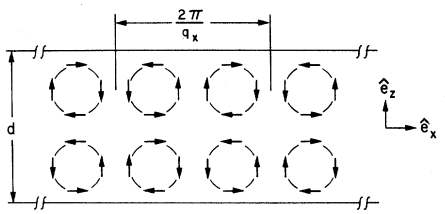

FIG. 5. Schematic of fluid-flow pattern resulting from the second set of solutions in Fig. 3. Computer calculation of the amplitudes for the solution $V_0 = 16$ V, $\varphi = 3.099$ have been performed. This solution corresponds to two layers of antiparallel vortices. It is proposed in the text that the competition of this solution with the $V_0 = 16$V, $\varphi = 1.1785$ solution results in turbulence. Turbulence has been observed and is known as the dynamic scattering mode (Ref. 31).

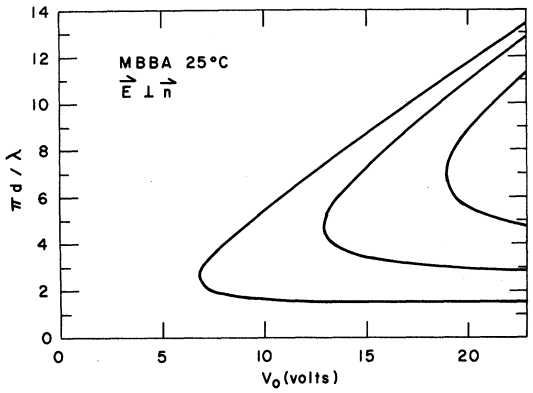

FIG. 6. Computer calculation of the normal-mode wave vectors for MBBA at 25 °C. The dispersion relations for MBBA are qualitatively similar to those for PAA (see Fig. 3). MBBA shows a slightly lower critical voltage of 6.9 V as compared to 8 V for PAA. The viscosities for MBBA are an order of magnitude larger than for PAA. Since the viscosities always enter the steady-state calculation in ratios [see Eq. (31)], the critical voltage is not strongly affected by the larger viscosity. As with Fig. 3, these curves may be altered somewhat by nonlinear effects.

presented by Helfrich.[18] One assumes a sinusoidal director-orientation dependence as given in Eq. (22). As was shown in Eq. (25), this leads to off-diagonal conductivity-tensor elements. It follows that E_x and D_x field components are nonzero and that $\nabla \cdot \vec{D}$ is not zero. There is a net space-charge density which can interact with the applied field. This interaction, in a stress-tensor representation is given by terms such as $D_x E_x$, i.e., the Maxwell stress tensor. This shear is opposed by elastic and viscous forces. At a critical voltage, the electric forces are sufficient to overcome the restoring-forces and fluid-motion results. Unfortunately we cannot offer a clear physical explanation for the critical voltage, and we must refer to the mathematical solution.

Since a large number of assumptions have been made in our treatment of the domain problem, it will be useful to make a unified statement of these assumptions: (i) negligible temperature gradients; (ii) $\alpha_1 = 0$; (iii) negligible electro- or magnetostriction; (iv) zero gravitational potential; (v) steady-state conditions; (vi) linearity in distortion amplitudes and distortion gradients; (vii) fluid-field equations (1)–(7); (viii) constitutive equations (8)–(15); and (ix) boundary conditions (16)–(19). As was mentioned above, assumptions 5 and 6 seem to be the best place to begin in future improvements of the theory. It is possible to measure θ_1 as a function of V_0, so a nonlinear theory could be quickly compared with experiment.[21]

CONCLUSION

We have developed a set of consistent differential equations [Eqs. (1)–(7)] for the description of electromagnetic effects in anisotropic liquids. The forces and torques exerted on the fluid by an electromagnetic field in a susceptible medium have been expressed in terms of operations on the Maxwell stress tensor. Solution of these general equations requires constitutive relationships. We have presented the standard set applicable to a NLC [Eqs. (8)–(15)].

The boundary-value problem associated with the Williams domain mode has been solved by using standard constitutive relations and experimentally determined material constants. We have demonstrated excellent agreement between the qualitative features of theory and experiment and satisfactory agreement on the quantitative features. We believe that this agreement proves the experimental validity of Carr's proposal[32] and Helfrich's original treatment[18] of conduction-induced alignment.

Note added in proof. S. A. Pikin {Zh. Eksperim. i Teor. Fiz. 60, 1185 (1971) [Sov. Phys. JETP 33, 641 (1971)]} has developed a theoretical treatment which is similar to the approach described here. He chose to derive approximate formulae for the critical voltage region. Thus his result is the demonstration of a critical voltage.

ACKNOWLEDGMENTS

We wish to thank Dr. W. Weber for valuable assistance in the numerical computations associated with this paper. We also gratefully acknowledge the MBBA material constants k_{11} and k_{33} provided by Dr. I. Haller.

APPENDIX A

This Appendix contains the demonstration that if the director $\vec{n}$ specifies the orientation of the uniaxial tensor $\overleftrightarrow{\epsilon}$, then the Maxwell stress tensor is of such a form that the vector $M_i = \epsilon_{ijk} T_{jk}$ has no finite component parallel to $\vec{n}$, i.e., $\vec{n} \cdot \vec{M} = 0$. For convenience we look at the problem in a coordinate system where $\vec{n}$ defines the x axis. Thus we have

$$\overleftrightarrow{\epsilon} = \begin{pmatrix} \epsilon_{\parallel} & 0 & 0 \\ 0 & \epsilon_{\perp} & 0 \\ 0 & 0 & \epsilon_{\perp} \end{pmatrix} \tag{A1}$$

The Maxwell stress tensor can be directly written down as

$$\overleftrightarrow{T} = \begin{pmatrix} T_{xx} & E_x E_y \epsilon_{\perp} \epsilon_0 & E_x E_z \epsilon_{\perp} \epsilon_0 \\ E_y E_x \epsilon_{\parallel} \epsilon_0 & T_{yy} & E_y E_z \epsilon_{\perp} \epsilon_0 \\ E_z E_x \epsilon_{\parallel} \epsilon_0 & E_z E_y \epsilon_{\perp} \epsilon_0 & T_{zz} \end{pmatrix}, \tag{A2}$$

where the elements T_{xx}, T_{yy}, and T_{zz} have not been written down explicitly, because they do not influence this proof. The vector M has the x component

$$M_x = \epsilon_{xjk} T_{jk} = (E_y E_z \epsilon_\perp - E_z E_y \epsilon_\perp)\, \epsilon_0 = 0 \,. \qquad \text{(A3)}$$

The dot product $(\vec{n} \cdot \vec{M})$ is exactly $n_x M_x$ which by (A3) is zero. Thus M can be written uniquely as a cross product of $\vec{n}$ and another vector.

APPENDIX B

The following experimental values of the material constants (PAA) were used in the domain calculation: $k_{11} = 7 \times 10^{-12}$ N at 120 °C (Ref. 33), $k_{33} = 17 \times 10^{-12}$ N at 120 °C (Ref. 33), $\epsilon_\parallel = 5.62$ at 120 °C (Ref. 34), $\epsilon_\perp = 5.83$ at 120 °C (Ref. 34), $\eta_1 = 1.5 \times 10^{-3}$ kg m^{-1} sec^{-1} at 125 °C (Ref. 35), $\eta_2 = 8.6 \times 10^{-3}$ kg m^{-1} sec^{-1} at 125 °C (Ref. 35), $\alpha_2 = -6.4 \times 10^{-3}$ kg m^{-1} sec^{-1} at 125 °C (Ref. 35), $\alpha_3 = -0.6 \times 10^{-3}$ kg m^{-1} sec^{-1} at 125 °C (Ref. 35), $\sigma_\parallel / \sigma_\perp = 1.5$ (estimate, Ref. 36).

APPENDIX C

The following MBBA material constants were used in the domain calculation for Fig. 6. The neumatic isotropic transition temperature was assumed to be 45 °C. The sample temperature was assumed to be 25 °C. We have the following: $k_{11} = 6.10 \times 10^{-12}$ N (Ref. 37), $k_{33} = 7.25 \times 10^{-12}$ N (Ref. 37), $\epsilon_\parallel = 4.72$ (Ref. 38), $\epsilon_\perp = 5.25$ (Ref. 38), $\eta_1 = 23.8 \times 10^{-3}$ kg m^{-1} sec^{-1} (Ref. 39), $\eta_2 = 103.5 \times 10^{-3}$ kg m^{-1} sec^{-1} (Ref. 39), $\alpha_2 = -77.5 \times 10^{-3}$ kg m^{-1} sec^{-1} (Ref. 39), $\alpha_3 = -1.2 \times 10^{-3}$ kg m^{-1} sec^{-1} (Ref. 39), $\sigma_\parallel / \sigma_\perp = 1.5$ (Ref. 38).

---

*Present address: Research Laboratory, Texas Instruments Inc., Dallas, Tex. 75222.

[1]G. H. Heilmeier, Sci. Am. 222, No. 4, 100 (1970).
[2]P. G. DeGennes, Solid State Commun. 6, 163 (1968).
[3]R. B. Meyer, Appl. Phys. Letters 12, 281 (1968).
[4]R. Williams, J. Chem. Phys. 39, 384 (1963).
[5]R. Aris, *Vectors, Tensors, and the Basic Equations of Fluid Mechanics* (Prentice-Hall, Englewood Cliffs, N. J., 1962).
[6]I. G. Chistyakov, Usp. Fiz. Nauk 89, 563 (1966) [Sov. Phys. Usp. 9, 551 (1967)].
[7]F. M. Leslie, Quart. J. Mech. Appl. Math. 19, 357 (1966).
[8]P. C. Martin, P. S. Pershan, and J. Swift, Phys. Rev. Letters 25, 844 (1970).
[9]D. Forster, T. C. Lubensky, P. C. Martin, J. Swift, and P. S. Pershan, Phys. Rev. Letters 26, 1016 (1971).
[10]H. Huang, Phys. Rev. Letters 26, 1525 (1971).
[11]L. D. Landau and E. M. Lifshitz, *Electrodynamics of Continuous Media* (Pergamon, Oxford, England, 1960), p. 64.
[12]W. K. H. Panofsky and M. Phillips, *Classical Electricity and Magnetism* (Addison-Wesley, Reading, Mass., 1962), p. 105.
[13]L. Spitzer, *Physics of Fully Ionized Gases* (Interscience, New York, 1962), p. 27.
[14]R. Becker and F. Sauter, *Electromagnetic Fields and Interactions* (Blaisdell Co., New York, 1964), Vol. I, p. 296.
[15]O. Parodi, J. Phys. (Paris) 31, 581 (1970).
[16]F. C. Frank, Discussions Faraday Soc. 25, 19 (1958).
[17]W. Helfrich, J. Chem. Phys. 51, 2755 (1969).
[18]W. Helfrich. J. Chem. Phys. 51, 4092 (1969).
[19]G. Durand, M. Veyssie, F. Rondelez, and L. Leger, Compt. Rend. 270B, 97 (1970).
[20]P. A. Penz, Phys. Rev. Letters 24, 1405 (1970); 25, 489 (1970).
[21]P. A. Penz, Mol. Cryst. 15, 141 (1971).
[22]N. Felici, Rev. Gen. Elec. 78, 717 (1969).
[23]J. M. Schneider and P. K. Watson, Phys. Fluids 13, 1948 (1970).
[24]M. Papoular, Phys. Letters 30A, 5 (1969).
[25]G. H. Heilmeier and W. Helfrich, Appl. Phys. Letters 16, 155 (1970).
[26]Orsay Liquid Crystal Group, Mol. Cryst. 12, 251 (1971).
[27]E. Dubois-Violette, P. G. de Gennes, and O. Parodi, J. Phys. (Paris) 32, 305 (1971).
[28]W. Greubel and U. Wolff, Appl. Phys. Letters 19, 213 (1971).
[29]L. K. Vistin, Dokl. Akad. Nauk SSSR 194, 1318 (1970) [Sov. Phys. Doklady 15, 908 (1971)]
[30]L. D. Landau and E. M. Lifshitz, *Fluid Mechanics* (Pergamon, London, 1959), p. 102.
[31]G. H. Heilmeier, L. A. Zanoni, and L. A. Barton, Proc. IEEE 56, 1162 (1968).
[32]E. F. Carr, Advan. Chem. Ser. 63, 76 (1967).
[33]A. Saupe, Z. Naturforsch. 15a, 815 (1960).
[34]W. Maier and G. Meier, Z. Naturforsch. 16a, 470 (1961); 16a, 1200 (1961).
[35]Orsay Liquid Crystal Group, Mol. Cryst. 13, 187 (1971).
[36]R. P. Twitchell and E. F. Carr, J. Chem. Phys. 46, 2765 (1967).
[37]I. Haller (private communication).
[38]D. Diguet, F. Kondelez, and G. Durand, Compt. Rend. 271B, 954 (1970).
[39]G. Gahwiller, Phys. Letters 36A, 311 (1971). We have changed the definitions used in this reference to correspond with the notation in Ref. 24.